

# New type of $B$ -periodic magneto-oscillations in a two-dimensional electron system induced by microwave irradiation

I. V. Kukushkin\*, M. Yu. Akimov\*, J. H. Smet, S. A. Mikhailov, K. von Klitzing  
*Max-Planck-Institut für Festkörperforschung, Heisenbergstr. 1, D-70569 Stuttgart, Germany*

I. L. Aleiner,  
*Physics Department, Columbia University, New York, NY 10027*

V. I. Falko  
*Department of Physics, Lancaster University, Lancaster LA1 4YB, UK*  
(Dated: October 30, 2018)

We observe a new type of magneto-oscillations in the photovoltage and the longitudinal resistance of a two-dimensional electron system. The oscillations are induced by microwave irradiation and are periodic in magnetic field. The period is determined by the microwave frequency, the electron density, and the distance between potential probes. The phenomenon is accounted for by coherent excitation of edge magnetoplasmons in the regions near the contacts and offers perspectives for the development of new tunable microwave and terahertz detection schemes and spectroscopic techniques.

Studies of two-dimensional electron systems (2DES) have revealed a variety of magneto-oscillations of both classical and quantum nature. The quantization of the energy spectrum into Landau levels manifests itself in  $1/B$ -periodic Shubnikov-de Haas oscillations [1] and in the quantum Hall effect [2]. Other examples of  $1/B$ -periodic oscillations include magnetophonon resonances, geometrical commensurability effects between the cyclotron radius and the period of a potential modulation [3], as well as the recently discovered microwave-induced zero-resistance states in high-mobility heterostructures, which are governed by the ratio of the microwave frequency  $\omega$  to the cyclotron frequency  $\omega_c$  in the regime  $\omega > \omega_c$  [4, 5, 6, 7, 8]. There also exist magnetotransport phenomena that yield  $B$ -periodic oscillations, such as the quantum Aharonov-Bohm effect and the classical effect of ballistic electron focusing between point contacts [9, 10].

In this Letter, we report the observation of a new type of  $B$ -periodic magnetotransport oscillations in GaAs/AlGaAs quantum wells. The effect is observed under incident microwave radiation when  $\omega < \omega_c$  (in contrast to the work in Refs. [4, 5, 6, 7, 8]) and consists of an oscillatory magnetic field dependence of the microwave-induced photovoltage and the resistance. The oscillation period  $\Delta B \propto n_s/\omega L$  depends on the microwave frequency  $\omega$ , the electron density  $n_s$ , and the distance between potential probes  $L$  placed along the long side of the Hall-bar sample. We interpret the observed oscillations as the manifestation of interference between edge magnetoplasmons (EMPs) [11, 12, 13, 14, 15, 16, 17, 18, 19, 20, 21, 22, 23, 24, 25, 26], coherently emitted from the near-contact regions under the influence of microwaves. The effect was observed in samples with macroscopic distances between contacts ( $\sim 1$  mm), in moderate fields (below 1–3 T), and across a wide range of microwave frequencies and temperatures (up to 70 K). This makes it a promising candidate for conceiving tunable microwave and terahertz detectors as well as spectrometers.

Several samples were processed from the same heterostructure into Hall-bar geometries with differing width  $W$  (0.4 mm and 0.5 mm) and distance between adjacent potential probes  $L$  (1.6 mm, 0.5 mm, 0.4 mm and 0.2 mm). In the dark, the electron concentration and mobility were approximately equal to  $1.6 \times 10^{11} \text{ cm}^{-2}$  and  $6 \times 10^5 \text{ cm}^2/\text{Vs}$ . In the majority of cases, a brief initial exposure of the sample to white light was necessary to bring out the  $B$ -periodic oscillations under incident microwave radiation. After exposure to white light, the density increased up to  $3.3 \times 10^{11} \text{ cm}^{-2}$  and the mobility improved to  $1.3 \times 10^6 \text{ cm}^2/\text{Vs}$ . The sample was placed in an oversized 16 mm waveguide at the maximum of the microwave electric field. Generators covered frequencies from 12 GHz to 58 GHz with input powers up to 1 mW. A sinusoidal current between 0.1 and 1  $\mu\text{A}$  with a frequency of 12 Hz is driven through the sample. For these amplitudes ohmic behavior was satisfied. The microwave power was modulated with 2 kHz. The double modulation technique enables us to measure both the influence of microwaves on the magnetoresistance (at 12 Hz) as well as the photovoltage (at 2 kHz). Control experiments verified that the same photovoltage was generated in the absence of an imposed current and that magnetoresis-

\*on leave from the Institute of Solid State Physics, Russian Academy of Sciences, Chernogolovka, Russia

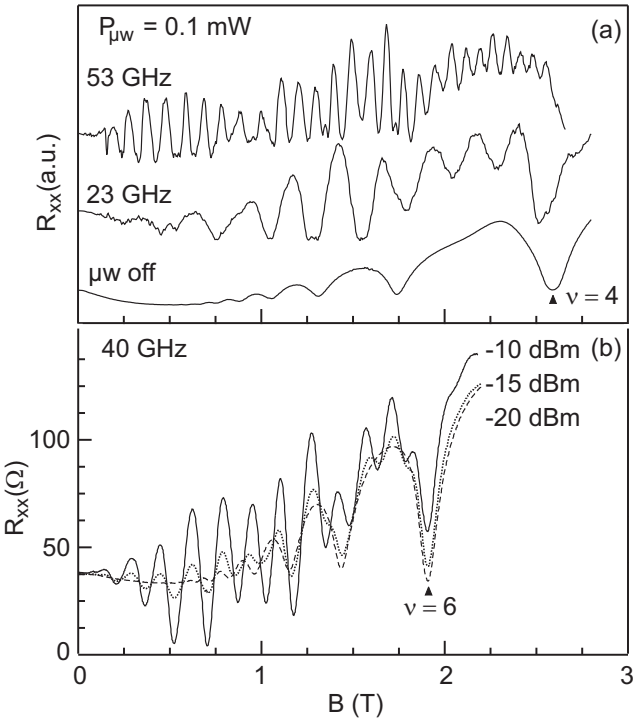


FIG. 1: (a) Longitudinal resistance  $R_{xx}$  as a function of magnetic field  $B$  without microwaves (the lower curve) and in the presence of microwaves for two different frequencies at the electron density  $n_s = 2.5 \times 10^{11} \text{ cm}^{-2}$  (the arrow marks Landau-level filling factor  $\nu = 4$ ). (b) Evolution of  $R_{xx}$  vs.  $B$  with microwave power  $P_{\mu w}$  (from bottom to top: 10, 30, and 100  $\mu W$ ) at  $n_s = 2.75 \times 10^{11} \text{ cm}^{-2}$ . The temperature  $T = 4.2$  K and the distance between the contacts  $L = 0.5$  mm are the same for both plots.

stance oscillations occurred for cw-microwave radiation.

Figure 1a shows the magnetic field dependence of the longitudinal resistance measured without and with microwave irradiation for frequencies of 23 and 53 GHz. Apart from the  $1/B$ -periodic SdH-oscillations, additional  $B$ -periodic oscillations emerge under incident microwave radiation. Their period is inversely proportional to the microwave frequency. Figure 1b illustrates the microwave-power dependence of the effect and shows that the power level does not affect the period of the oscillations, but greatly influences their amplitude. In Figure 2 the oscillation maxima have been assigned an index  $N$  and their magnetic field position is plotted. The  $B$ -periodic behavior is obvious and holds for a wide range of microwave frequencies (at least from 12 GHz to 58 GHz). At low microwave frequencies, where the waveguide only supports a single mode, the influence of the microwave polarization has been investigated. The amplitude of the oscillations is far stronger for a microwave electric field perpendicular to the current direction. Moreover, a threshold behavior as a function of microwave power is apparent. The threshold power value is lower for mi-

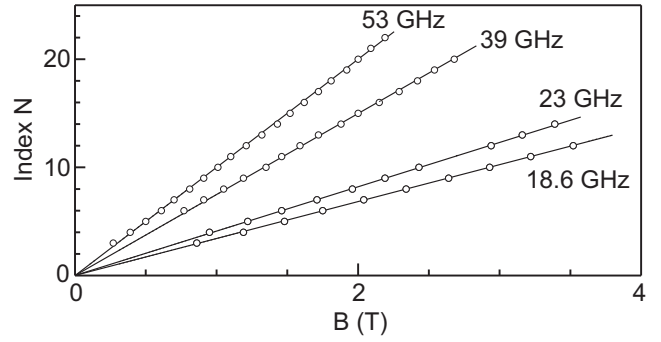


FIG. 2: Oscillation maxima are assigned an integer index  $N$ . Their magnetic field position is plotted versus the index for various microwave frequencies. The electron density is equal to  $2.61 \times 10^{11} \text{ cm}^{-2}$ , the distance  $L = 0.5$  mm.

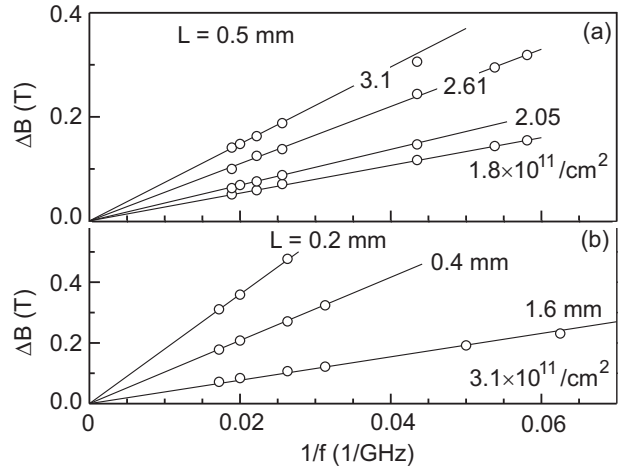


FIG. 3: (a) The period  $\Delta B$  of the oscillations versus inverse microwave frequency for various electron concentrations at  $L = 0.5$  mm. (b)  $\Delta B$  versus  $1/f$  for different distances between potential contacts and  $n_s = 3.1 \times 10^{11} \text{ cm}^{-2}$ .

crowave radiation polarized perpendicular to the long direction of the Hall bar. Furthermore, the oscillation period is independent of temperature  $T$ . Also the amplitude only weakly drops upon increasing  $T$  from 1.5 to 10 K. Figure 3 illustrates in more detail how the oscillation period  $\Delta B$  (extracted from a Fast-Fourier-Transform analysis) depends on microwave frequency as well as the electron density.  $\Delta B$  goes with the inverse of the frequency and superlinearly increases with density. It was also established that  $\Delta B$  is approximately proportional to the inverse distance between potential probes  $L$  (see Fig 3b).

In addition to the oscillations in the longitudinal resistance, also an oscillating voltage difference  $V_{xx}$  appears across any voltage contact pair along the side of the Hall bar. The  $B$ -periodicity (see Figure 4) of  $R_{xx}$  and  $V_{xx}$  is identical (although with a  $1/4$ -period phase shift) and suggests a similar physical origin for both effects. Yet,

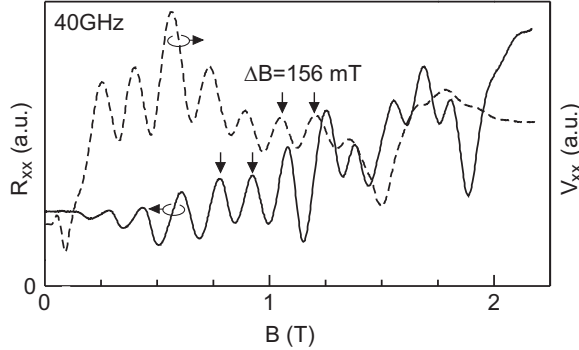


FIG. 4: Magnetoresistance  $R_{xx}$  and photovoltaic  $V_{xx}$  versus applied magnetic field for 40 GHz incident microwave radiation,  $n_s = 2.75 \times 10^{11} \text{ cm}^{-2}$ ,  $L = 0.5 \text{ mm}$ , and a sample current of  $1 \mu\text{A}$ .

the microwave power and the temperature dependencies of their amplitude is quite distinct. The amplitude of the photovoltaic oscillations is linear in the microwave power without a threshold and saturates at a value of approximately 2 mV for 0.1 mW of power. This value is close to the threshold power of the resistance oscillations. In addition, the photovoltaic effect is even less sensitive to temperature and drops only by approximately one order of magnitude when raising the temperature to 70 K.

The dependence of the period  $\Delta B$  on microwave frequency, electron density and distance between potential contacts suggests that the effect is related to the excitation of EMPs in the vicinity of potential probes. EMPs are plasma waves propagating along the edge of the 2DES in the direction dictated by the external magnetic field orientation [11, 12, 13, 14, 15, 16, 17, 18, 19, 20, 21, 22, 23, 24, 25, 26]. Their velocity is proportional to the Hall conductivity  $\sigma_{yx} \propto n_s/B$  of the 2DES. Hence, assuming that their wavevector is given by  $2\pi N/L$  with integer  $N$ , one immediately finds the qualitatively correct dependencies  $\Delta B \propto n_s/\omega L$ .

Now, we consider the phenomenon in more detail. The inset to Fig. 5 schematically shows the near-contact region in our samples. The contact may be regarded as a piece of wire of width  $w$  attached to the 2DES. The oscillating external electric field  $\mathbf{E}(t) = \mathbf{E}_0 e^{-i\omega t}$  induces an oscillating current inside the wire and produces oscillating line charges near its sides, with the linear charge density  $\rho$  estimated as [27]

$$\rho = \frac{\sigma_{yx}(\omega)E_x^0 + \sigma_{yy}(\omega)E_y^0}{i\omega\zeta(\omega)}. \quad (1)$$

Here  $\sigma_{\alpha\beta}(\omega)$  is the dynamical conductivity tensor,  $\zeta(\omega) = 1 - \omega_p^2/(\omega^2 - \omega_c^2) \approx 1 + \omega_p^2/\omega_c^2$  the dielectric response function, and  $\omega_p$  the plasma frequency of the wire ( $\omega_p^2 \propto n_s/w$ ). Because the potential probes violate the translational invariance of the 2DES edge, they create oscil-

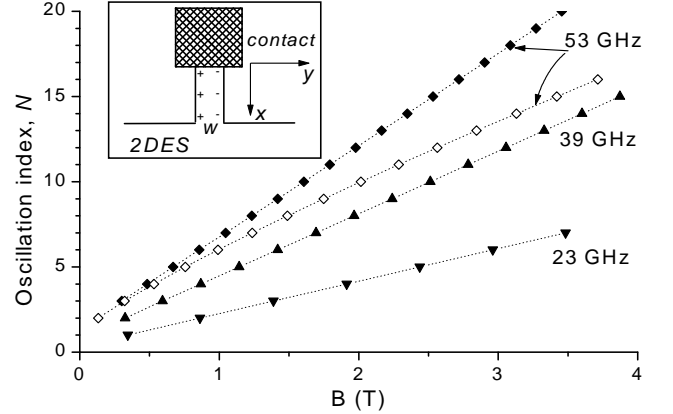


FIG. 5: The oscillation index  $N$  calculated from the dispersion equation  $D(2\pi N/L, \omega) = 0$  as a function of magnetic field for parameters of our samples  $n_s = 2.61 \times 10^{11} \text{ cm}^{-2}$ ,  $L = d_2 = 0.5 \text{ mm}$ , and  $d_1 = 0.21 \mu\text{m}$  (solid symbols). The curve with open symbols is plotted for  $f = 53 \text{ GHz}$  and  $d_1 = 0 \mu\text{m}$  (no cover layer). The inset schematically illustrates the distribution of microwave-induced charges near contacts.

lating dipoles, which serve as antennas emitting EMPs. The frequency of the excited EMPs equals the microwave frequency  $\omega$ , and their wavevector  $q_y$  is determined from the dispersion equation  $D(q_y, \omega) = 0$ , where [24]

$$D(q_y, \omega) = \frac{i|q_y|\sigma_{xx}(\omega)}{q_y\sigma_{yx}(\omega)} - \tanh \left\{ \int_0^{\pi/2} \ln \epsilon \left( \frac{|q_y|}{\sin t}, \omega \right) \frac{dt}{\pi} \right\}. \quad (2)$$

Here, we have assumed a sharp, step-like equilibrium density profile  $n_s(x) = n_s\theta(x)$  and

$$\epsilon(q, \omega) = 1 + \frac{4\pi i\sigma_{xx}(\omega)q}{\omega\kappa \left[ \frac{\kappa \tanh qd_1 + 1}{\kappa + \tanh qd_1} + \frac{\kappa \tanh qd_2 + 1}{\kappa + \tanh qd_2} \right]} \quad (3)$$

is the wave-vector and frequency dependent dielectric function of the system composed of (i) the dielectric substrate with thickness  $d_2$  and dielectric constant  $\kappa$ , (ii) the 2D electron layer and (iii) cover layers with total thickness  $d_1$  and dielectric constant  $\kappa$  made up of the AlGaAs-spacer, the dopant and usual capping layers.

The excitation of coherent EMPs by two adjacent contacts on the same side of the Hall bar a distance  $L$  apart may be in phase or out of phase depending on the wavevector  $q_y$  of the EMPs. If the chiral EMP exiting the left contact propagates to the right, it may constructively interfere with the EMP injected by the second contact provided that the travelled distance  $L$  is such that  $q_y L$  takes on a multiple of  $2\pi$ . The amplitude of the combined wave propagating to the right from the second contact will thus oscillate as a function of  $q_y L$ , with maxima/minima occurring each time when  $q_y L = 2\pi N$ . In the experiment, this manifests itself through the observed magneto-oscillations of the photovoltaic and the photoresistance. We calculate the ‘oscillation index’  $N$  as a

function of magnetic field by solving the EMP dispersion equation  $D(2\pi N/L, \omega) = 0$  numerically under the assumption of a collisionless Drude model for  $\sigma_{\alpha\beta}(\omega)$ . The results (Figure 5, solid symbols) demonstrate a nearly ideal linear dependence  $N(B)$ . The slope of the  $N(B)$  curves is somewhat smaller than in experiment (Figure 2), which implies that the ‘theoretical’ EMPs are running faster than in experiment. There are two factors which may help to explain this quantitative discrepancy: inaccurate descriptions of the dielectric environment surrounding the 2DES and the equilibrium density profile  $n_s(x)$ . The curve with open symbols in Figure 5 for  $d_1 = 0$  demonstrates for instance the importance of including a very thin, but non-zero thickness cover layer. It substantially improves agreement between theory and experiment both in terms of the linearity and slope. Incorporating the presence of metallic pieces around the sample (conducting wires, the waveguide), as well as a more realistic density profile  $n_s(x)$  with soft walls (smoothed over a  $\mu\text{m}$ -scale length [18, 19, 20, 21]) will further reduce the EMP velocity and improve the agreement.

The validity of the EMP-based interpretation was additionally tested by measuring the photovoltaic on a sequence of three potential probes (1, 2 and 3) on the same side of the Hall bar in positive and negative  $B$ -fields. Due to the chiral nature of EMPs, the observed photovoltaic oscillations for a given orientation of  $B$  were stronger between contacts (2,3) and smaller for the potential probe pair (1,2). When inverting the  $B$ -field orientation, the EMP propagation direction is concomitantly reversed and the oscillations now indeed become pronounced between contacts (1,2) instead and weak for probe pair (2,3). Also the polarization dependence of the effect is consistent with the proposed model. Since at high magnetic fields  $\sigma_{yx} \gg \sigma_{yy}$ , the amplitude of the EMP emitting dipoles, Eq. (1), is much stronger for microwave fields polarized across the Hall bar in agreement with observations.

A quantitative microscopic model for non-linearities, which enable the detection of EMPs through a measurement of the induced photovoltaic and photoresistance, is yet to be developed. Qualitatively, the photovoltaic effect may be caused by rectification of the oscillating EMP field in the potential probes and/or by local *dc*-currents dragged along the edges by propagating EMP waves. Both mechanisms yield the linear dependence of the photovoltaic on microwave power. The non-linear power dependence of the photoresistance could be accounted for as follows. At low power levels, the oscillating EMP field causes a *dc*-voltage between potential probes, but does not significantly modify equilibrium properties of the 2DES such as for instance the density. At stronger microwave powers,  $n_s$  is locally altered (near the contacts) and the longitudinal resistance is affected. The same EMP-emission mechanism may therefore produce the  $B$ -periodic oscillations in  $R_{xx}$ , but only at large

enough microwave powers. The classical nature of EMPs explains why the effect is weakly influenced by  $T$  and why it is observable even at liquid nitrogen temperatures.

In summary, we have observed a novel type of  $B$ -periodic microwave-induced oscillations in the photovoltaic and the photoresistance of the 2DES. We ascribe them to the coherent excitation and interference of edge magnetoplasmons, which generate a non-linear response. The phenomenon was seen across a broad range of frequencies, in moderate magnetic fields and up to liquid nitrogen temperatures. It opens prospects for developing innovative microwave and terahertz detection schemes and spectroscopic techniques.

We acknowledge financial support from the Max-Planck and Humboldt Research Award, the Russian Fund of Fundamental Research, INTAS and the DFG. VF acknowledges support from EPSRC and the Royal Physical Society. VF and IK thank NATO CLG for funding their collaboration.

---

- [1] T. Ando, A. B. Fowler, and F. Stern, Rev. Mod. Phys. **54**, 437 (1982).
- [2] K. von Klitzing, G. Dorda, and M. Pepper, Phys. Rev. Lett. **45**, 494 (1980).
- [3] R. R. Gerhardts, D. Weiss, and K. von Klitzing, Phys. Rev. Lett. **62**, 1173 (1989).
- [4] M. A. Zudov, R. R. Du, J. A. Simmons, and J. L. Reno, Phys. Rev. B **64**, 201311 (2001).
- [5] P. D. Ye, L. W. Engel, D. C. Tsui, J. A. Simmons, J. R. Wendt, G. A. Vawter, and J. L. Reno, Appl. Phys. Lett. **79**, 2193 (2001).
- [6] R. G. Mani, J. H. Smet, K. von Klitzing, V. Narayananamurti, W. B. Johnson, and V. Umansky, Nature **420**, 646 (2002).
- [7] M. A. Zudov, R. R. Du, L. N. Pfeiffer, and K. W. West, Phys. Rev. Lett. **90**, 046807 (2003).
- [8] S. I. Dorozhkin, JETP Letters **77**, 577 (2003).
- [9] H. van Houten, B. J. van Wees, J. E. Mooij, C. W. J. Beenakker, J. G. Williamson, and C. T. Foxon, Europhys. Lett. **5**, 721 (1988).
- [10] C. W. J. Beenakker, H. van Houten, and B. J. van Wees, Europhys. Lett. **7**, 359 (1988).
- [11] D. B. Mast, A. J. Dahm, and A. L. Fetter, Phys. Rev. Lett. **54**, 1706 (1985).
- [12] D. C. Glattli, E. Y. Andrei, G. Deville, J. Poitrenaud, and F. I. B. Williams, Phys. Rev. Lett. **54**, 1710 (1985).
- [13] A. L. Fetter, Phys. Rev. B **32**, 7676 (1985).
- [14] A. L. Fetter, Phys. Rev. B **33**, 3717 (1986).
- [15] M. Wassermeier, J. Oshinowo, J. P. Kotthaus, A. H. MacDonald, C. T. Foxon, and J. J. Harris, Phys. Rev. B **41**, 10287 (1990).
- [16] R. C. Ashoori, H. L. Störmer, L. N. Pfeiffer, K. W. Baldwin, and K. West, Phys. Rev. B **45**, 3894 (1992).
- [17] V. K. Talyanskii, J. E. F. Frost, M. Pepper, D. A. Ritchie, M. Grimshaw, and G. A. C. Jones, J. Phys. Condens. Matter **5**, 7643 (1993).
- [18] N. B. Zhitenev, R. J. Haug, K. von Klitzing, and K. Eberl, Phys. Rev. Lett. **71**, 2292 (1993).

- [19] N. B. Zhitenev, R. J. Haug, K. von Klitzing, and K. Eberl, Phys. Rev. B **49**, 7809 (1994).
- [20] I. L. Aleiner and L. I. Glazman, Phys. Rev. Lett. **72**, 2935 (1994).
- [21] C. Dahl, S. Manus, J. P. Kotthaus, H. Nickel, and W. Schlapp, Appl. Phys. Lett. **66**, 2271 (1995).
- [22] V. A. Volkov and S. A. Mikhailov, Pis'ma Zh. Eksp. Teor. Fiz. **42**, 450 (1985), [JETP Lett. **42**, 556-560 (1985)].
- [23] V. A. Volkov, D. V. Galchenkov, L. A. Galchenkov, I. M. Grodnenskii, O. R. Matov, and S. A. Mikhailov, Pis'ma Zh. Eksp. Teor. Fiz. **44**, 510 (1986), [JETP Lett. **44**, 655-659 (1986)].
- [24] V. A. Volkov and S. A. Mikhailov, Zh. Eksp. Teor. Fiz. **94**, 217 (1988), [Sov. Phys.-JETP **67**, 1639-1653 (1988)].
- [25] V. A. Volkov and S. A. Mikhailov, in *Landau Level Spectroscopy*, edited by G. Landwehr and E. I. Rashba (North-Holland, Amsterdam, 1991), vol. 27.2 of *Modern Problems in Condensed Matter Sciences*, chap. 15, pp. 855-907.
- [26] S. A. Mikhailov, in *Edge Excitations of Low-Dimensional Charged Systems*, edited by O. Kirichek (Nova Science Publishers, Inc., NY, 2000), chap. 1, pp. 1-47.
- [27] S. A. Mikhailov, Pis'ma Zh. Eksp. Teor. Fiz. **57**, 570 (1993), [JETP Lett. **57**, 586-590 (1993)].